

Burst Grooming in Optical-Burst-Switched Networks

Sami Sheeshia and Chunming Qiao

Department of Computer Science & Engineering
State University of New York at Buffalo, Buffalo NY 14260
sheeshia@eng.buffalo.edu, qiao@computer.org

Abstract

We describe the problems and challenges of switching small bursts in Optical-Burst-Switched (OBS) networks especially when the burst size is small and comparable to the switching time. We propose extending OBS with input and output port (fiber) grooming capabilities and develop the corresponding fabric architectures. We also construct an approximate model to analyze the throughput and delay, and present results of various analytical and experimental studies. Our simulation results demonstrate that burst grooming yields switching gains as the throughput of groomed traffic in slow nodes can approach that of non-groomed traffic in faster nodes.

1. Introduction

Recently, Optical Burst Switching (OBS) has been the subject of intense research in the academia [1] and industry [2][3] because it provides statistical multiplexing of network resources and is more efficient than circuit and packet switching. Unlike circuit-switched transports such as Optical Circuit Switching and Next-Generation SONET, OBS reserves core wavelengths for the duration of data bursts thereby allowing wavelength sharing among different traffic flows. In addition, OBS avoids the complexities of Optical Packet Switching which requires large delay lines and fast electronic processing of packet headers, by processing the control information prior to data transmissions. OBS data bursts are transmitted on all-optical paths without requiring any O/E/O conversions in the network core. These paths are signaled using out-of-band control packets (CP) which are transmitted some offset time prior to data transmissions and processed electronically at every intermediate node. Edge data packets such as IP and Ethernet, are aggregated by destination and QoS parameters and transmitted in bursts of varying lengths. This burst elasticity makes OBS very efficient for transporting bursty asynchronous traffic as demonstrated in [4].

Due to the significant increase in IP and Ethernet traffic in the local and wide area networks, much of the current

research in OBS has focused on supporting asynchronous data traffic which tends to be large in size and tolerant of some delay and loss. However, this may not always be the case as protocol and synchronous data tend to be small in size and must be transported promptly using small bursts if necessary. These characteristics reduce the network utilization especially if the burst size is comparable to the switching time (that is the time required to setup the cross-connect).

The motivation for this paper is to expand the concept of burst grooming as reported in [5] and develop architectures that shift bursts with the same destination, closer in time in order to reduce the per-burst switching overhead and use the fewest switching operations possible. In addition to these objectives, grooming reduces the inter-burst gaps and recovers the additional channel void capacity which should lead to improved network utilization. The rest of the paper is organized as follows: Section 2 describes the general idea of burst grooming and presents our proposed schemes. Corresponding grooming architectures and equivalent network models are presented in Sections 3 and 4 respectively. We then analyze and formulate the grooming objective as a set of delay, and throughput optimization problems in Sections 5 and 6. The simulation setup is presented in Section 7 and the analytical and experimental results are discussed in Section 8. We then conclude this paper in Section 9 with a brief summary of our findings and future research direction.

2. Burst grooming

Formally, burst grooming is defined as the alignment of several bursts that have the same destination closer in time so they can be switched as one unit until they are separated again. Ideally, bursts that have the same next hop, as opposed to the same destination, should be groomed. However, this is very complex as burst grooming reduces the inter-burst gaps thus making it difficult to de-groom bursts at the next hop.

In our context, burst grooming refers to the grooming (as opposed to combining) of as many bursts that have the same destination as possible, regardless of their size and

without limiting the size of the groomed burst. We define an alternate type of grooming called *burst selective grooming* (BSG) where several bursts are groomed up to a maximum size limit; the size of the resulting groomed bursts cannot exceed an upper bound. Clearly, bursts that exceed this limit are not eligible for grooming but are switched separately.

We differentiate between two types of grooming techniques depending on where the bursts are re-arranged, input-port (or input fiber) and output-port grooming as shown in Figures 1 and 2. The main functional difference between the two is that in input-port grooming, incoming bursts are groomed before they are switched whereas in output-port grooming, bursts are switched first and then groomed at their output ports.

Output-port Grooming (OPG) re-aligns the bursts at the output ports of the node by using small Fiber Delay Lines (FDLs) to shift preceding bursts closer to succeeding bursts. Bursts from different input ports (or fibers) and different wavelengths are re-arranged at their designated output ports after they have been switched. An example is shown in Figure 1 where bursts 1 and 2 are first converted to the appropriate wavelength, switched, and then shifted (or delayed) in the FDLs of port 3 closer to bursts 4 and 3 respectively. Note that OPG provides for cross-port grooming where bursts from different input fibers can be groomed together as well as cross-wavelength grooming within the same fiber where bursts 1 and 2 can be groomed with bursts 3 and 4 instead. As such, the reduction in switching operations in OPG is not realized at the grooming node itself but rather at downstream nodes.

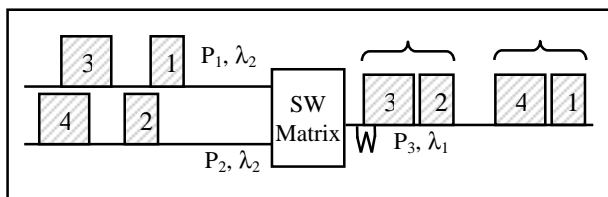


Figure 1. Output port based grooming

Input-port Grooming (IPG) re-arranges bursts at the input ports prior to the switching matrix. Incoming bursts are intercepted and delayed in FDLs at each input port, just enough so they can be switched with succeeding bursts. An example is shown in Figure 2 where normally four (2 per ingress wavelength) switching operations will be required. Instead, the grooming algorithm delays bursts 1 and 2 just enough to allow one switching operation per ingress wavelength instead of two. As such, the reduction in switching operations in IPG is realized immediately at the grooming node.

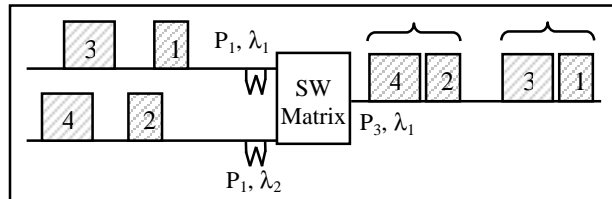


Figure 2. Input port based grooming

OPG is simpler and preferred to IPG for several reasons. First, burst scheduling algorithms can easily incorporate burst grooming as an objective. For example, the scheduling algorithm assigns the burst to the egress wavelength which results in the smallest inter-burst gap after the burst undergoes some delay. As such, OPG can take advantage of the switch node capabilities, FDLs and wavelength converters (WC), and requires less hardware and control. Second, OPG is not limited to core nodes but can be implemented at edge nodes where newly assembled bursts are delayed in electronic RAM (instead of FDLs) and groomed with transit bursts.

In many respects, OPG and IPG are not mutually exclusive but are complementary; bursts that cannot be groomed using OPG at the output ports, due to lack of FDLs for example, are transmitted separately and groomed at the input of the downstream node using IPG.

3. Grooming architectures

We present two possible grooming architectures for the OPG and IPG modules that can be integrated within the OBS node itself, either on the fiber port card or at the input-output of the switch matrix. We use these architectures to develop equivalent network models for analysis in later sections and note that regardless of the architecture, grooming requires the splitting, delaying, and merging of bursts, which reduces the signal power and limits the scalability of the architecture.

3.1. OPG architecture

The fabric of the OPG module consists of banks of small feed-forward FDLs on each egress port as shown in Figure 3. Bursts that arrive at the OPG module have already been assigned to the appropriate egress wavelength. As a result, the module's architecture is simple but the control must be incorporated into the scheduling algorithm because grooming alters the channel voids and scheduling horizon.

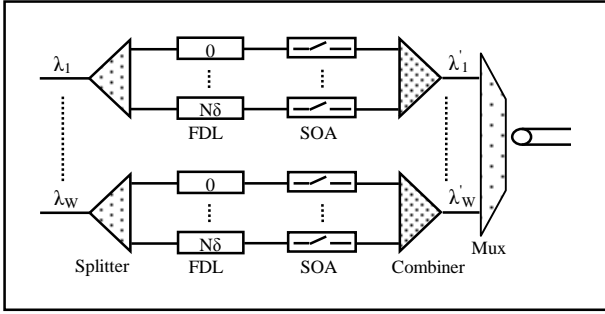


Figure 3. OPG module architecture

A signal (burst) arriving on a particular wavelength at the module is split into $N+1$ duplicate signals and delayed in N FDLs with δ granularity. Appropriately delayed bursts are then selected using *Semiconductor Optical Amplifier* (SOA) gates and combined to form larger bursts at the output whereas the duplicate bursts are simply discarded. Note that SOA gates are *on/off* switches that connect one port to another and do not incur the setup penalties as the switching matrix does.

3.2. IPG architecture

Figure 4 shows a possible 2-stage architecture of the grooming fabric that resembles the broadcast-and-select architecture discussed in [6] and [7]. The first stage consists of tunable WC and multi-granularity feed-forward FDLs whereas the second stage combines the bursts onto the appropriate wavelength prior to the switching matrix. Incoming signals are de-multiplexed into W wavelengths which may be converted to appropriate output wavelengths. These wavelengths are then split into N identical signals and fed into N FDLs with δ granularity. Each FDL output signal is again split into W signals, one per output wavelength, where SOA gates in the second stage select the appropriately delayed bursts; other duplicate bursts are discarded.

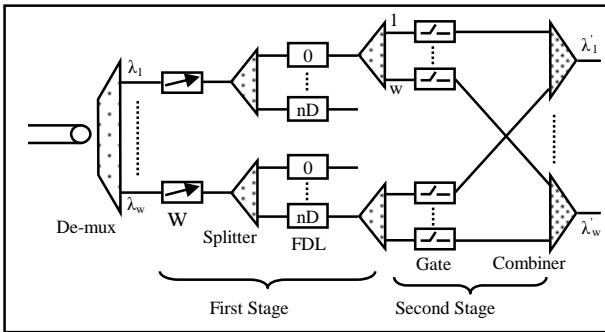


Figure 4. IPG module architecture

This architecture does not lend itself to cross-port (or cross-fiber) grooming at the input due to the number of

splitters and SOA gates that will be required. IPG's limited scalability restricts its functionality to grooming bursts across multiple wavelengths of the same input fiber only.

4. Equivalent models

We derive equivalent network models for the IPG and OPG modules in order to analyze the average grooming delay and blocking probability. We note that the only functional difference between the IPG and OPG modules is that a burst that enters the IPG module may be converted to a different wavelength prior to switching whereas in OPG, WC is a function of the burst scheduler and not the OPG module itself.

4.1. OPG model

The OPG module of Figure 3 is modeled in Figure 5 where a burst arrival on wavelength i with rate λ_i (not shown in Figure 5) is converted to a different wavelength j by the scheduling algorithm with probability β_{ij} and requires a grooming delay of $n\delta$ with probability α_{jn} . Consequently, the mean of the cumulative arrival rate of the egress wavelength j is $\lambda'_j = \sum_i \sum_n \beta_{ij} \alpha_{jn} \lambda_i$ and accounts for the scheduling procedure.

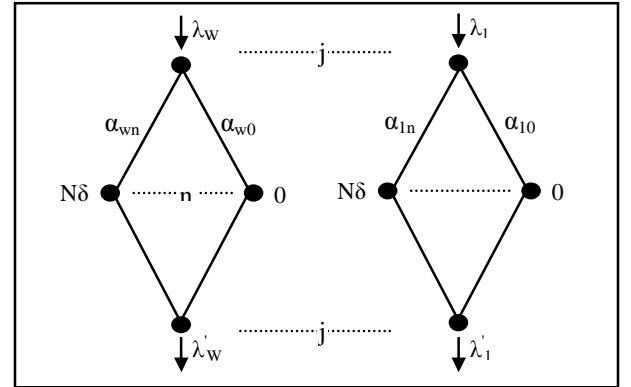


Figure 5. OPG equivalent model

4.2. IPG model

The equivalent network model of the IPG architecture of Figure 4 is shown in where an arrival on ingress wavelength i with rate λ_i requires a delay of $n\delta$ with probability α_{in} and gets converted to wavelength j with probability β_{nj} . The mean of the cumulative arrival rate at wavelength j prior to switching is $\lambda'_j = \sum_i \sum_n \alpha_{in} \beta_{nj} \lambda_i$.

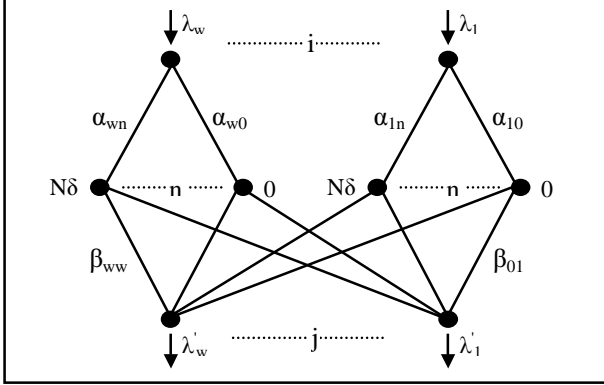


Figure 6. IPG equivalent model

5. Analytical model

We first note the similarity between the OPG and IPG cumulative arrival rate λ_j and conclude that the IPG model of Figure 6 can be used to evaluate the performance of the IPG module alone or the performance of the burst scheduler with OPG. For our purposes, we limit the analysis to the IPG model using the notations in Table 1.

Table 1. Notations for the analysis

Term	Description
T_x	Switching time
W	Number of wavelengths per port (fiber)
N	Number of FDL units per wavelength
n	Index of FDL unit (1..N)
i (j)	Index of ingress (egress) wavelength, (1..W)
μ	Mean service rate
L	Mean burst length ($1/\mu$)
Λ	Total arrival rate
λ	Mean arrival rate of a single stream
γ	Mean throughput
α_{in}	Routing probability from i to FDL n
β_{nj}	Routing probability from FDL n to j
λ_i	Mean arrival rate of wavelength i
λ_j	Mean arrival rate at wavelength j
λ_{ij}	Mean arrival rate from i to j
λ_{ijn}	Mean arrival rate from i to j through FDL n
δ	FDL granularity
D_n	Delay of FDL n
g	Inter-burst gap length
$f(g)$	Inter-burst gap length distribution
P_g	Probability of a burst being groomed
D_g	Mean grooming delay
P_j	Mean blocking probability of wavelength j
P_b	Mean blocking probability

We consider exponential burst arrival and lengths with mean arrival rate λ bursts/sec and L respectively, to derive the probability of a burst undergoing grooming, the average delay, and blocking probability.

5.1. Probability of Grooming (P_g)

With exponential arrivals, the gap length (g) between two consecutive bursts of a single stream, has a mean

$$E[g] = \frac{1}{\lambda} - L \text{ and a distribution}$$

$$f(g) = \begin{cases} 0 & \frac{1}{\lambda} \leq L \\ \frac{\lambda}{1-\lambda L} e^{-\frac{\lambda}{1-\lambda L} g} & \text{Otherwise} \end{cases} \quad (1)$$

P_g is derived from $f(g)$ where in general, a burst is groomed with its consecutive burst if their inter-burst gap g is larger than the switching time T_x

$$P_g = P[g > T_x] = \begin{cases} 0 & \frac{1}{\lambda} \leq L \\ e^{-\frac{\lambda T_x}{1-\lambda L}} \cong \frac{1-\lambda L}{1-\lambda(L-T_x)} & \text{Otherwise} \end{cases} \quad (2)$$

More generally, Equations (1) and (2) can be extended to account for the superposition of multiple streams and wavelengths, as will be the case with wavelength conversion, by replacing λ with the total (cumulative) arrival rate $\Lambda = \sum_i \lambda_i$. Also note that Equation (2) does

not account for the probability that a burst will be groomed with its n^{th} succeeding burst.

5.2. Average Grooming Delay (D_g)

A burst from an ingress wavelength may traverse any of the N FDLs depending on its inter-burst gap g with its succeeding burst. Using Equation (2), the per-stream average burst delay is

$$\begin{aligned} D_g &= 0P(g < \delta) + \dots + n\delta P(n\delta \leq g < (n+1)\delta) \\ &= \sum_n n\delta P(n\delta \leq g < (n+1)\delta) \\ &= \sum_n n\delta \left(e^{-\frac{\lambda \delta n}{1-\lambda L}} - e^{-\frac{\lambda \delta (n+1)}{1-\lambda L}} \right) \end{aligned} \quad (3)$$

where λ can be replaced with Λ to derive the average grooming delay across all input streams and wavelengths.

5.3. Wavelength Blocking Probability (P_j)

We assume that blocking is solely due to contentions resulting from two or more bursts contending for the same egress wavelength j , and do not consider blocking across the splitter junctions or the switching matrix. In general, a burst is dropped if it arrives at wavelength j during the service time of another burst. Therefore, the blocking probability of wavelength j is

$$P_j = \sum_i \sum_n P(\text{Server } j \text{ is busy due to } \lambda_{ijn}) \cdot P(\text{Burst arrives from another } \lambda_{ijn}) \quad (4)$$

Using the gap length distribution of Equation (1), we can estimate P_j with

$$P_j = \sum_i \sum_n \left(\frac{\lambda_{ijn}}{\mu} \right) \left(\frac{1}{1 + \left(\sum_i \sum_k (\lambda_{ijk}) - \lambda_{ijn} \right) / \mu} \right) \quad (5)$$

P_j can be further simplified by replacing the arrival rate λ_{ijn} with the cumulative arrival rate λ'_j to give

$$\lambda'_j = \sum_i \sum_n \lambda_{ijn} = \sum_i \sum_n \alpha_{in} \beta_{nj} \lambda_i \quad (6)$$

$$P_j = \sum_i \sum_n \left(\frac{\lambda_{ijn}}{\mu + \lambda'_j - \lambda_{ijn}} \right) \cong \sum_i \sum_n \frac{\lambda_{ijn}}{\mu + \lambda'_j} = \frac{\lambda'_j}{\mu + \lambda'_j} \quad (7)$$

Equation (7) is the blocking probability of a M/M/1/1 queue. It follows that the grooming module can be modeled as an M/M/W/W queue where the total blocking probability P_b is

$$P_b = \frac{\sum_i \lambda_i}{W\mu + \sum_i \lambda_i} \quad (8)$$

and the average throughput γ is

$$\gamma = \sum_i \lambda_i (1 - P_b) \quad (9)$$

Note that in Equation (7), the approximation of $\lambda'_j - \lambda_{ijn}$ with λ'_j is justified because $\lambda'_j = \sum_i \sum_n \lambda_{ijn} \gg \lambda_{ijn}$; in other words, the cumulative arrival rate at wavelength j from all ingress wavelengths i through all FDLs n , is larger than the arrival rate from one ingress wavelength through one FDL.

6. Optimization Routines

The burst grooming problem is formulated as a set of non-linear (NLP) optimization routines with the objective of minimizing the average delay and maximizing the throughput. In these formulations, we ignore the switching time to derive the theoretical bounds of the objectives and note that the objective of maximizing the throughput is equivalent to minimizing the inter-burst gaps.

6.1. Delay Minimization

The delay minimization objective can be stated as:

$$\text{Objective: Min } \sum_i \sum_j \sum_n D_n \alpha_{in} \beta_{nj} \frac{\lambda_i}{\Lambda}$$

Subject To:

1. $\sum_i \sum_n \lambda_i \alpha_{in} \beta_{nj} \leq \mu$ for all j
2. $\sum_n \sum_j \alpha_{in} \beta_{nj} \leq 1$ for all i
3. $\sum_n \alpha_{in} = 1$ for all i
4. $\sum_j \beta_{nj} = 1$ for all n

where the delay for FDL n $D_n = n\delta$ and the total offered traffic is $\Lambda = \sum_i \lambda_i$. Constraint (1) guarantees that the

egress wavelength capacity is not exceeded whereas constraint (2) states that if a burst of wavelength i is assigned to FDL n , then it must be assigned to one egress wavelength j . Constraints (3) and (4) guarantee that a burst is assigned to one FDL n and one egress wavelength j respectively.

6.2. Throughput Maximization

Using the constraints of the delay routine, the throughput objective is formulated as:

$$\text{Objective: Max } \sum_j \frac{\lambda'_j}{\Lambda}$$

Subject To:

1. $\sum_i \sum_n \alpha_{in} \beta_{nj} \lambda_i \leq \mu$ for all j
2. $\sum_n \sum_j \alpha_{in} \beta_{nj} \leq 1$ for all i
3. $\sum_n \alpha_{in} = 1$ for all i
4. $\sum_j \beta_{nj} = 1$ for all n

where the cumulative arrival rate to wavelength j is $\lambda'_j = \sum_i \sum_n \alpha_{in} \beta_{nj} \lambda_i$ and $\Lambda = \sum_i \lambda_i$ is the total offered traffic.

7. Experimental Setup

It is clear that burst grooming will improve the switching efficiency at the expense of additional delays. However, what is not readily clear is its impact on throughput. We evaluate this impact by simulating a single OBS node with eight wavelengths per fiber, and wavelength conversion and IPG capabilities. The node is modeled using OPNET [8] and simulated with and without grooming for various traffic loads.

The traffic model consists of a single class of traffic with exponentially distributed burst lengths and inter-arrival times. The average burst length is $L = 5000$ bytes and the average arrival rate Λ bursts/sec is determined from the offered load.

In this study, burst grooming is simulated by having the scheduling algorithm periodically batch process a number of sorted CPs starting with the latest arriving bursts to the earliest; in other words, the latest arriving bursts are scheduled first. Other bursts that result in the smallest inter-burst gaps using the least amount of delays possible are then scheduled on the appropriate channels. Note that the objective of this heuristic algorithm is to maximize the throughput of each channel by compacting its schedule using the smallest delays possible. Alternatively, although not implemented in this simulation, the heuristic can be modified to emphasize the delay objective by selecting the bursts that require the smallest delays but do not necessarily result in the smallest inter-burst gaps. For the non-grooming scenario, the latest available unscheduled channel with void filling scheduling algorithm [9] is used.

For the grooming process, we first permit as many bursts as possible to be groomed together which results in large groomed bursts. We then rerun the simulation with BSG and arbitrarily set the limit on the maximum size of the groomed burst (i.e. the number of bytes that can be groomed together) to 20 Kbytes (or an average of 4 bursts). Bursts whose sizes exceed this limit are not groomed with other bursts.

In addition, a simulation of non-groomed traffic in an OBS node with half the switching time (i.e. twice as fast) is carried out to compare the throughput of the non-groomed traffic with that of the groomed traffic in the slower node.

8. Results and Discussion

The weighted sum method is used to combine the two optimization routines into one function which is then modeled and solved using AMPL and PENNON [10]. In order to select the set of weights that result in the closest performance to the simulation results, the function is solved using three sets of delay and throughput weights, w_d and w_t respectively. The first set emphasizes the delay objective by setting w_d to 0.9 and w_t to 0.1. The second set emphasizes the throughput objective by setting w_d to 0.1 and w_t to 0.9. The third set weighs the two objectives equally, $w_d=w_t=0.5$. The corresponding delay and throughput results are shown in Figures 7 and 8 where it can be observed that the third set of equal weights achieves a good tradeoff between delay and throughput and a close match to the simulation results.

We first note that the delay and throughput optimization results represent the optimal values and theoretical bounds that can be achieved by IPG for the given set of weights whereas the analytical results represent the average delay and throughput values when consecutive bursts are groomed. As such, we do not expect the optimization and analytical results to be consistent with one another.

Next we compare the performance of the groomed with the non-groomed traffic using the simulation results in order to quantify the additional IPG delay and throughput gains. It is clear from Figure 7 that groomed traffic will incur additional delays due to the shifting and re-aligning of bursts closer to each other. Fortunately, the simulation results show that this additional delay is small and fairly constant for traffic loads below 80 percent. For loads above 80 percent, the increase in the average delay is due to the rapid increase in the groomed burst size which creates more contentions. As a result, non-groomed bursts incur higher delays as they are shifted onto other wavelengths. However in general, the delay results of Figure 7 demonstrate that burst grooming does not have a significant impact on delay.

As for the throughput performance, the simulation results in Figure 8 show that for loads less than 88 percent, groomed traffic has higher throughput (~2 percent) than non-groomed traffic. This is because burst grooming compacts the channel schedules and results in larger voids that can be filled with additional bursts, as opposed to channel voids that are too small to fit other bursts. Alternatively, this increase in throughput implies that for a given load, a node with grooming capabilities requires fewer wavelengths than a node without grooming. For loads higher than 88 percent however, grooming can cause excessive contentions as larger bursts make it exceedingly difficult to schedule smaller bursts and are themselves prone to more contentions. As a result, the groomed traffic

has lower throughput at high loads than the non-groomed traffic.

The previous conclusion indicates that at high loads, there is a trade-off between grooming and throughput; larger groomed bursts improve the switch utilization and reduce the number of switching operations required, but result in more scheduling contentions than smaller bursts. A possible solution is to limit the size of the groomed burst by using BSG. As shown in Figure 8, for loads above 76 percent, the BSG traffic has about 3 percent higher throughput than non-BSG groomed traffic but lower throughput at lower loads. This is because the size limit on the groomed burst reduces contentions at high loads but does not completely compact the channel voids at low loads.

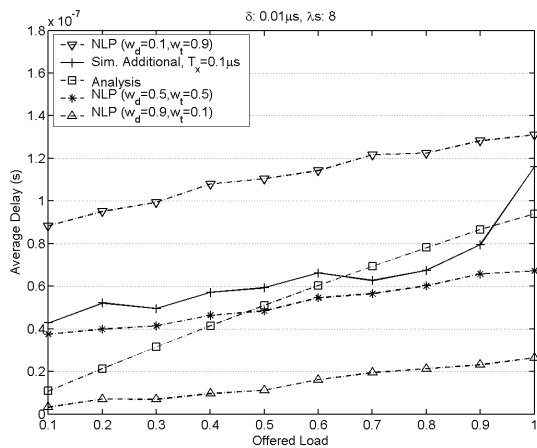


Figure 7. Average IPG delay

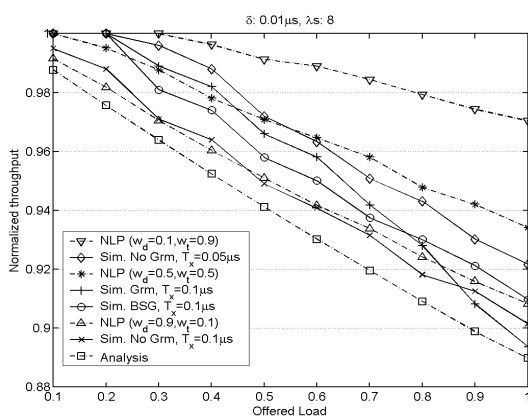


Figure 8. Average IPG throughput

Also shown in Figure 8 are the throughput results of a faster node (or smaller switching time) without grooming. Observe that for loads below 70 percent, the throughput of the groomed traffic in the slow node is very close to the throughput of the non-groomed traffic of the faster node.

This indicates that a node with grooming capabilities can emulate a node that is nearly twice as fast. However, for loads above 70 percent, the two graphs diverge, which again demonstrates that non-BSG grooming has adverse effects on throughput at high loads whereas BSG does not.

These results show that in order for burst grooming to maintain high network throughput at all loads, an adaptive grooming procedure must be used to account for the input traffic load and vary the groomed burst size limit accordingly.

9. Conclusion

In this paper, we have presented the concept of burst-level grooming in OBS as a means of increasing the per-wavelength utilization and the switching efficiency. We have highlighted input and output port grooming strategies, discussed their advantages and disadvantages, and presented corresponding architectures. We note that output-based grooming is preferred to input-based grooming due to its cross-port functionality and scalability. We have also developed equivalent analytical models for the average delay and throughput, and demonstrated that grooming improves throughput for some traffic loads at the expense of additional delays. However at high traffic loads, the groomed burst size must be limited by using burst selective grooming in order to keep contentions at an acceptable level. As a result, such grooming techniques can save on wavelength resources and yield a throughput performance that is similar to that of a faster node, and perhaps at a much lesser cost.

We conclude by noting that grooming is not limited to burst-switched networks but can be applied to packet-based transports in order to compensate for slow switching. Developing adaptive and more efficient grooming algorithms and architectures that provide burst multiplexing and de-multiplexing functionality in the OBS core, as in hop-based instead of destination-based grooming, are open to further research.

10. References

- [1] C. Qiao and M. Yoo, "Choices, features, and issues in optical burst switching (OBS)", *Optical Networking Mag.*, April 2000, pp. 36-44.
- [2] L. Sofman and T. El-Bawab, Alcatel USA, "Segmentation overhead in optical burst switching", *Optical Networking and Communication Conference*, July-August 2002, pp. 4874-09.
- [3] S. Ovidia, C. Maciocco, and M. Paniccia, Intel Corporation, "GMPLS-Based Photonic Burst Switching (PBS) Architecture for Optical Networks", Available:

<http://www.cse.buffalo.edu/~qiao/wobs/wobs2003/files/WOBS110%20FINAL.pdf>

[4]S. Sheeshia and C. Qiao, "Supporting Ethernet in optical-burst-switched networks", *J. Optical Networking*, vol. 1, no. 8/9, 2002, pp. 299-312.

[5]S. Sheeshia and C. Qiao, "Synchronous Optical Burst Switching", *Broadnets*, Oct. 2004.

[6]M. Renaud, F. Masetti, C. Guillemot, and B. Bostica, "Network and system concepts for optical packet switching", *IEEE Commun. Mag.*, vol. 35, no. 4, 1997, pp. 96-102.

[7]C. Guillemot, "Transparent optical packet switching: The European Acts KEOPS project approach", *J. Lightwave Technology*, vol. 16, no. 16, 1998, pp. 2117-2134.

[8]<http://www.opnet.com>

[9]Y. Xiong, M. Vandenhoute, and H. Cankaya, "Control Architecture in Optical Burst-Switched WDM Networks", *IEEE J. Select Areas Commun.*, vol. 18, Oct. 2000, pp. 1838-1851.

[10] <http://www.ampl.com>